Growth kinetics engineered magnetoresistance response in La2/3Sr1/3MnO3 thin films

A. Pomar,[1] J. Santiso,[2] F. Sandiumenge,[1] J. Roqueta,[2] B. Bozzo,[1] C. Frontera,[1] Ll. Balcells,[1] B. Martínez,[1] and Z. Konstantinović[1]

[1]*Institut de Ciència de Materials de Barcelona–CSIC, Campus de la UAB, 08193 Bellaterra, Spain*
[2]*Institut Català de Nanociència i Nanotecnologia, ICN2 (CSIC, CERCA). Campus de la UAB, 08193 Bellaterra, Spain*

A route to engineer the intrinsic colossal magnetoresistance (CMR) response in manganite thin films through an accurate control of the growth kinetics is presented. It is shown that under specific growth conditions, a particular strained state, substantially different from that of bulk-like materials and standard films, can be quenched up to film thicknesses around 60 nm. This strained state exhibits the same structural fingerprints of the interfacial dead layer in standard films and promotes surface morphology instabilities, which end up with the formation of self-organized nanopits array. At the same time, it has profound effects on the intrinsic magnetoelectronic properties of the films that exhibit an enhanced intrinsic CMR response. © *2014 AIP Publishing LLC*. [http://dx.doi.org/10.1063/1.4871984]

From a technological point of view, optimally doped La2/3Sr1/3MnO3 (LSMO) is the most interesting compound of the manganite perovskite family due to its Curie temperature well above room temperature that makes its fascinating physical properties suitable for practical applications.[1] However, in bulk state, LSMO only shows appreciable magnetoresistance (MR) at high fields around the transition temperature.[2] In recent years, there have been several attempts to improve the colossal MR (CMR) response of LSMO, mainly at low fields, to fit within the requirements for useful technological applications. LSMO, having a broad bandwidth and a quite stable ferromagnetic phase, does not present electronic phase separation, as observed in other narrow bandwidth manganite perovskites,[3] which restricts the possible mechanisms for tuning the intrinsic CMR response. Nevertheless, extrinsic magnetoresistance can be properly modified by engineered grain boundaries[4–9] in nanocomposite thin films. In these systems, extrinsic magnetoresistance, governed by spin-polarized tunneling across grain boundaries, could be significantly enhanced at low fields. In fact, MR values around 25% have been reported at low temperatures (10 K) and H = 0.5 T.[6] However, as mentioned above, enhancing the intrinsic CMR response seems to be more challenging.

An interesting approach has recently emerged by taking advantage of the strong coupling existing in these compounds between lattice, charge, orbital, and spin degrees of freedom. It is well known that the ferromagnetic/metallic state in manganite thin films can be modified by lattice perturbations through epitaxial strains.[2] This has been used by several groups to explore the effect of strain on the intrinsic CMR response of LSMO thin films and significant enhancements have been reported (64% at H = 5 T).[10–13] Strain-stabilized structural phase coexistence at low temperature was suggested as a possible mechanism for the observed CMR increase.[12] Similarly, analogous arguments may also be invoked to explain not only the CMR increase but also the anomalous behavior of the magnetotransport properties

of a few unit cells thick LSMO films, where competing interactions promote electronic phase separation and stabilize an insulating phase, usually referred to as dead-layer.[14–20] This tuning of the electronic properties has been mainly explored by changing the strained state of the film through lattice mismatch with the substrate.[10,13] The present work is devoted to explore an approach based of the effects of growth kinetics on the delicate balance between electronic and structural degrees of freedom. We will show that by properly choosing the growth conditions, films may exhibit strained states inaccessible in bulk form with enhanced CMR response.

In this paper, we study the magnetotransport properties of LSMO thin films grown under specific conditions to promote the appearance of nanostructured surface morphologies, in particular, the spontaneous formation of self-organized nanopits arrays.[21,22] An investigation of the growth mechanism of such films[23] indicates that nanopits result from a kinetically driven surface instability encompassing the stabilization of interfacial lattice distortions[20] up to large film thicknesses. We will show that such films, hereafter referred to as nanostructured thin films (NTFs), present a high CMR response with values in excess of 40% at 1 T and above 90% at 9 T over a broad range of temperatures.

Epitaxial LSMO NTFs with thicknesses varying between 8 nm and 200 nm were grown by RF magnetron sputtering[21,22,24] at 900 °C under a pure oxygen pressure of 19 Pa. Argon gas was not used during deposition process. Voltage bias of 120 V was chosen to obtain a growth rate of 1 nm min^{-1}. Since the miscut angle of the substrate plays an important role on the surface nanostructuring process, all NTFs used in this study were grown on a unique SrTiO3 (STO) (001) substrate. The substrate was cut in several pieces, typically 1×5 mm^2, and submitted to the standard thermal treatment to guarantee a single chemical surface TiO2 termination.[22] In addition, reference LSMO films grown under standard conditions to obtain flat surfaces with single unit cell step terraces were also prepared.[20] The surface morphology was investigated by atomic force microscopy (AFM)

and scanning electron microscopy (SEM). A typical image of the surface of a 17 nm thick NTF featuring self-organized nanopits is shown in the inset of Fig. 1(a). Structural properties were studied by X-ray diffraction (XRD). Measurements with synchrotron radiation were carried out at the KMC2 beamline at Helmholtz-Zentrum Berlin. Magnetotransport measurements were carried out in a standard four-probe configuration. Platinum contacts (10 nm thick) were evaporated through appropriate shadow masks. Measurements were performed in a Physical Properties Measurement System between 10 K and 400 K with perpendicular applied magnetic field up to 9 T. The main result of this work is displayed in Figs. 1(a) and 1(b), where magnetotransport properties of a 17 nm thick NTF are plotted in comparison with those of a reference flat LSMO film. From Fig. 1(a), it is observed that the NTF exhibits a much higher resistivity value (near one order of magnitude higher at room temperature) and a downward shift of the metal-to-insulator transition temperature ($T_{MI} \sim 150$ K). In the presence of magnetic fields, the resistance of the NTF is reduced over the whole range of temperatures and the maximum shifts upwards to higher temperatures giving rise to a CMR response, which achieves its maximum around the transition temperature. A huge increase of the magnetoresistance in the whole range of applied fields is detected in the NTF case, as shown in Figure 1(b), where R_H/R_0 is plotted around the corresponding T_{MI} for each sample. Both the upwards shift of the maximum of the R(T) curve with magnetic field and the monotonous field dependence of the R(H) curves are clearly in contrast with the typical features of grain boundary enhanced MR observed in granular materials, i.e., a sharp rise at very low fields (H < 0.5 T) followed by a strong change of slope in the R(H) curve and no shift of the maximum of the R(T) curves with field.[4] Moreover, all microstructural studies performed in our samples did not show any signature of significant granularity, and no grain boundaries were observed around the formation of nanopits.[24] The results in Figure 1 and the fact that MR maximum lays around T_{MI} disregard any contribution of granularity[3] and suggest an effective enhancement of the intrinsic CMR in these films.

In the simplest double exchange picture of mixed-valence manganites, CMR is considered to occur when the system is close to the metal-insulator transition, and the magnetic field strongly enhances ferromagnetic correlations in the insulating phase promoting the transition to the ferromagnetic-metallic phase with the corresponding huge decrease of the resistance. Tuning of this process has been usually explored by modifying the doping rate or even by varying the optimal oxygen content, which alters the Mn^{3+}/Mn^{4+} ratio. However, according to the double exchange picture, the CMR response can also be modified by acting on some physical parameters such as Mn-O-Mn bond angle and bond distances. Fortunately, in thin films, this can be accomplished in a relatively easy manner through epitaxial strain. Epitaxial strain may modify the electronic hopping amplitude not only by changing the Mn-O-Mn bond angle and Mn-O length but also by altering the Jahn-Teller orbital splitting and thus favouring the tendency to electronic localization.[25,26] There are several reports in the literature showing an efficient enhancement of CMR for LSMO thin films grown on substrates imposing a large epitaxial strain such as $LaAlO_3$, $DyScO_3$, or $GdScO_3$.[10,13] Conversely, for small misfit values, as in the case of (100) STO substrates (tensile strain of $\varepsilon \sim 0.6\%$), no enhancement of the CMR has been observed.[10] However, elastic strain is not the only ingredient in the recipe and, indeed, insulating behaviour has been repeatedly reported for ultra thin LSMO grown on STO substrates.[14–20] This insulating phase appears as the result of a misfit relaxation scenario where electronic distortion is the dominant mechanism over purely elastic strain or octahedral tilting mechanisms.[20] In NTFs, the strain relaxation mechanism is modified in such a way that the electronic distortion persists up to much larger thicknesses than in flat films. Interestingly, strain relaxation through surface instabilities leading to the formation of self-assembled nanopits seems to lock an unusual LSMO strained state with strong implications on the magnetotransport properties of the system.

As determined from X-ray measurements, similarly to flat films,[20] NTFs are strained with the in-plane lattice parameter matching that of the underlying STO substrate (a = 0.3905 nm) up to large thicknesses. In contrast, the measured c-axis parameter has been found to be unexpectedly large. For example, c = 0.3879 nm was measured in the 17 nm thick film, yielding an anomalously small Poisson ratio $\nu \sim 0.03$, much smaller than that obtained for flat films in the elastically strained rhombohedral state,[20] $\nu \sim 0.33$ ($\nu = \varepsilon^{\perp}/(\varepsilon^{\perp}-2\varepsilon^{\parallel})$, where $\varepsilon^{\perp}$ and $\varepsilon^{\parallel}$ are the out-of-plane and in-plane strain components, respectively ($a_{bulk} = 0.3881$ nm (Ref. 27) is used as a reference value). Moreover, the detailed analysis of X-ray reciprocal space maps (see Figure 2(a)) shows that contrary to twinned flat films, which reveal a clear splitting associated to (100) and (010) twins,[20] NTFs do not exhibit a fully developed rhombohedral phase, as indicated by the large spread of the film peak intensity along both the Q_x and Q_y axes. The diamond shape of the intensity contour lines suggests an incipient stage in the development of the rhombohedral shear strain along the [100] and [010] directions.[28] During the growth of LSMO on STO, the electronic and structural interaction at the interface induces the formation of a Mn^{3+} enriched monoclinically distorted
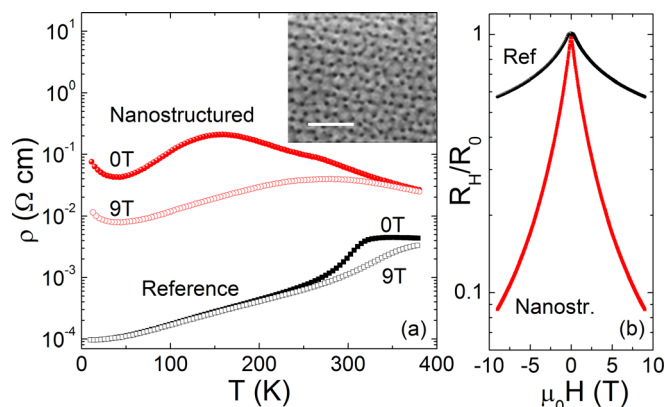

FIG. 1. (a) Temperature dependence of the electrical resistivity of a 17 nm thick LSMO nanostructured film (red circles) and a reference (flat surface) LSMO film (black squares). (b) Field dependence of resistivity of the films in (a) around their respective temperature transition. Inset in (a) shows a SEM image of the surface of the LSMO nanostructured film. Scale bar corresponds to 500 nm.
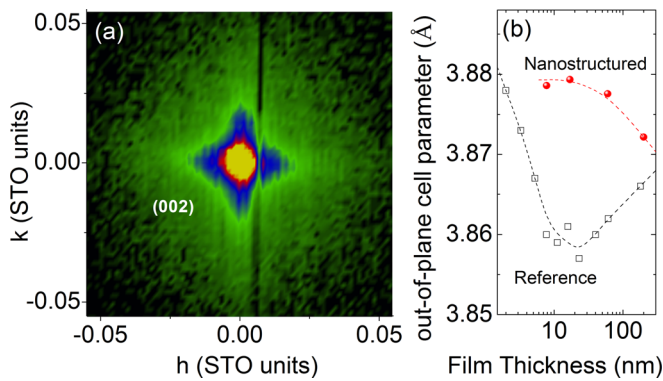
FIG. 2. (a) Reciprocal space map around the (002) reflection of a 17 nm thick nanostructured LSMO thin film. (b) Evolution with thickness of the out-of-plane cell parameter as determined from x-ray measurements for nanostructured (closed symbols) LSMO thin films. For comparison, results of reference films taken from Ref. 20 are also plotted. Lines are guides for the eyes.

~2.5 nm thick interfacial layer, exhibiting an anomalously large c-axis parameter and depressed magnetotransport properties.[14] Therefore, it appears that the structural and magnetotransport features of NTFs resemble those characterizing the interfacial dead layer in flat films. A comparison between the thickness dependence of the c-axis parameter of flat films[20] and NTFs (see Fig. 2(b)) clearly shows that the anomalous high values persist in the NTFs up to much higher thicknesses. Altogether, our magnetotransport and structure results strongly point that under the present growth conditions, the same mechanism that promotes the formation of surface nanopits also hinders the full transformation of the monoclinically distorted interfacial layer to the equilibrium rhombohedral phase. The continuous intensity spread along Q_x and Q_y strongly suggests that the films retain a complex microstructure with a subtle modulation of the Mn-O-Mn path at the nanoscale that hinders the development of the double exchange ferromagnetic phase explaining the observed enhancement of CMR.

Figures 3(a) and 3(b) show the temperature dependence of the magnetoresistance defined as MR(%) = (ρ(T,H)-ρ(T,0))/ρ(T,0) × 100, for H = 1 T and for H = 9 T, respectively. For comparison, we have also plotted the magnetoresistance of a standard 40 nm thick flat LSMO film as a solid line in both figures. Whereas in flat LSMO thin films above 10–15 nm, there is almost no appreciable influence of the thickness on their magnetotransport properties,[29] here we may observe that the magnetoresistance is gradually reduced as film thickness increases. Concomitantly, the maximum in MR is shifted towards higher temperatures following the same trend as the corresponding transition temperature. For a thickness of 200 nm, the magnetotransport properties are similar to those observed in standard LSMO thin films (see black lines in Fig. 1) although at H = 9 T there is still a significant magnetoresistance in the low temperature region. Note also that the transition temperature is well above room temperature probing that the nominal oxygen pressure is not a determinant parameter in the results here presented.

Annealing effects on the magnetotransport properties of NTFs were also performed to check the robustness of this strained state. Under annealings up to relatively high temperatures (~700 °C), NTF retained their enhanced CMR
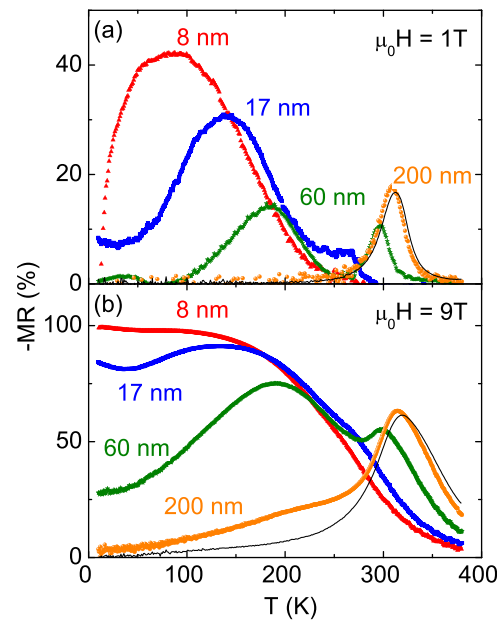

FIG. 3. Temperature dependence of the magnetoresistance for nanostructured LSMO films with different thicknesses at applied magnetic fields of (a) 1 T and (b) 9 T.

response. A significant evolution of the properties was only observed when annealings were performed at conditions approaching the growth temperature. Fig. 4(a) shows the temperature dependence of the MR at 1 T of the as-grown 17 nm thick NTF (closed red symbols) and after an annealing in oxygen atmosphere at 900 °C for 1 h (open black symbols). It is observed that after annealing, the LSMO film recovers the bulk-like behaviour (compare with the black line in Fig. 3), exhibiting only a modest MR, not bigger than 15%, around the transition temperature, now shifted above 300 K. The electrical conductivity has also been improved at all temperatures (see inset in Fig. 4(a)). At the same time, annealed films tend to exhibit a flatter surface morphology.[24] This implies that the strained state has relaxed towards a more standard LSMO bulk-like phase. This change can be monitored as well by measuring the c-axis parameter of the as-grown and annealed films. As shown in Fig. 4(b), a reduction of the c-axis parameter is detected in the annealed film
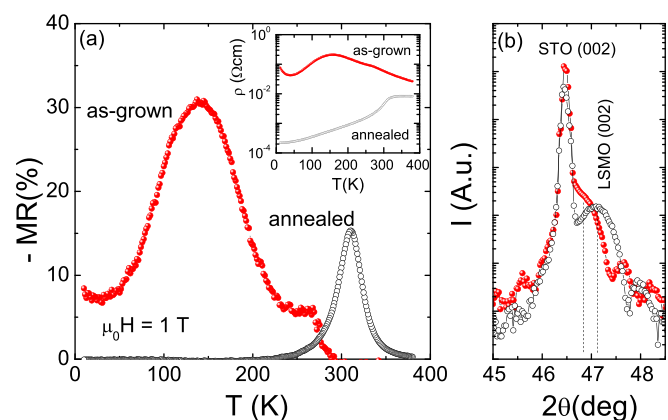

FIG. 4. (a) Magnetoresistance and electrical resistivity (inset) of a nanostructured LSMO thin film as-grown and after annealing at high temperature. (b) X-ray diffraction pattern around 002 peak of the same film in (a) reflecting the change in c-axis parameter after annealing.

($c_{annealed} \sim 0.3852$ nm and $c_{as\text{-}grown} \sim 0.3879$ nm), thus confirming that the modified strain state is responsible for the observed change of the magnetotransport properties.

In summary, we have shown experimental evidences of a route to engineer the colossal magnetoresistance response in manganite thin films through an accurate control of the growth kinetics. In this way, a balance between different competing strain relaxation mechanisms can be achieved, leading to a strained state substantially different from that of relaxed flat thin films or bulk-like materials. This strained state has a profound effect on the magnetotransport properties of the films due to a subtle modification of Mn-O-Mn bond angle and the Mn-O length and/or by altering the Jahn-Teller splitting, thus hindering the development of the double exchange ferromagnetic phase and favouring the tendency towards electronic localization. As a result, NTFs exhibit a behaviour close to that of lower doping rate compositions approaching the antiferromagnetic phase and prone to display electronic localization effects.

[1] A. Urushibara, Y. Moritomo, T. Arima, A. Asamitsu, G. Kido, and Y. Tokura, Phys. Rev. B **51**, 14103 (1995).

[2] Y. Tokura, Rep. Prog. Phys. **69**, 797 (2006).

[3] P. K. Siwach, H. K. Singh, and O. N. Srivastava, J. Phys.: Condens. Matter **20**, 273201 (2008).

[4] R. Gross, L. Alff, B. Buchner, B. H. Freitag, C. Hofener, J. Klein, Y. F. Lu, W. Mader, J. B. Philipp, M. S. R. Rao, P. Reutler, S. Ritter, S. Thienhaus, S. Uhlenbruck, and B. Wiedenhorst, J. Magn. Magn. Mater. **211**, 150 (2000).

[5] A. Gupta, G. Q. Gong, G. Xiao, P. R. Duncombe, P. Lecoeur, P. Trouilloud, Y. Y. Wang, V. P. Dravid, and J. Z. Sun, Phys. Rev. B **54**, R15629 (1996).

[6] A. P. Chen, Z. X. Bi, C. F. Tsai, J. Lee, Q. Su, X. H. Zhang, Q. X. Jia, J. L. MacManus-Driscoll, and H. Y. Wang, Adv. Funct. Mater. **21**, 2423 (2011).

[7] A. Chen, Z. Bi, C.-F. Tsai, L. Chen, Q. Su, X. Zhang, and H. Wang, Cryst. Growth Des. **11**, 5405 (2011).

[8] M. Staruch, D. Hires, A. Chen, Z. Bi, H. Wang, and M. Jain, J. Appl. Phys. **110**, 113913 (2011).

[9] M. Staruch, H. Gao, P.-X. Gao, and M. Jain, Adv. Funct. Mater. **22**, 3591 (2012).

[10] Y. Takamura, R. V. Chopdekar, E. Arenholz, and Y. Suzuki, Appl. Phys. Lett. **92**, 162504 (2008).

[11] C. Adamo, X. Ke, H. Q. Wang, H. L. Xin, T. Heeg, M. E. Hawley, W. Zander, J. Schubert, P. Schiffer, D. A. Muller, L. Maritato, and D. G. Schlom, Appl. Phys. Lett. **95**, 112504 (2009).

[12] S. Mukhopadhyay, I. Das, and S. Banerjee, J. Phys.: Condens. Matter **21**, 026017 (2009).

[13] F. J. Wong, S. Zhu, J. M. Iwata-Harms, and Y. Suzuki, J. Appl. Phys. **111**, 063920 (2012).

[14] J. Z. Sun, D. W. Abraham, R. A. Rao, and C. B. Eom, Appl. Phys. Lett. **74**, 3017 (1999).

[15] M. Huijben, L. W. Martin, Y. H. Chu, M. B. Holcomb, P. Yu, G. Rijnders, D. H. A. Blank, and R. Ramesh, Phys. Rev. B **78**, 094413 (2008).

[16] B. Kim, D. Kwon, T. Yajima, C. Bell, Y. Hikita, B. G. Kim, and H. Y. Hwang, Appl. Phys. Lett. **99**, 092513 (2011).

[17] H. Boschker, J. Kautz, E. P. Houwman, W. Siemons, D. H. A. Blank, M. Huijben, G. Koster, A. Vailionis, and G. Rijnders, Phys. Rev. Lett. **109**(5), 157207 (2012).

[18] C. Aruta, G. Ghiringhelli, A. Tebano, N. G. Boggio, N. B. Brookes, P. G. Medaglia, and G. Balestrino, Phys. Rev. B **73**, 235121 (2006).

[19] M.-B. Lepetit, B. Mercey, and C. Simon, Phys. Rev. Lett. **108**, 087202 (2012).

[20] F. Sandiumenge, J. Santiso, L. Balcells, Z. Konstantinović, J. Roqueta, A. Pomar, J. P. Espinos, and B. Martinez, Phys. Rev. Lett. **110**, 107206 (2013).

[21] Z. Konstantinović, J. Santiso, L. Balcells, and B. Martinez, Small **5**, 265 (2009).

[22] Z. Konstantinović, J. Santiso, D. Colson, A. Forget, L. I. Balcells, and B. Martinez, J. Appl. Phys. **105**, 063919 (2009).

[23] Z. Konstantinović, J. Santiso, L. Balcells, and B. Martinez, Nanotechnology **21**, 465601 (2010).

[24] Z. Konstantinović, F. Sandiumenge, J. Santiso, L. Balcells, and B. Martinez, Nanoscale **5**, 1001 (2013).

[25] A. J. Millis, T. Darling, and A. Migliori, J. Appl. Phys. **83**, 1588 (1998).

[26] A. Mukherjee, W. S. Cole, P. Woodward, M. Randeria, and N. Trivedi, Phys. Rev. Lett. **110**(15), 157201 (2013).

[27] P. G. Radaelli, G. Iannone, M. Marezio, H. Y. Hwang, S. W. Cheong, J. D. Jorgensen, and D. N. Argyriou, Phys. Rev. B **56**, 8265 (1997).

[28] J. Santiso, L. Balcells, Z. Konstantinović, J. Roqueta, P. Ferrer, A. Pomar, B. Martinez, and F. Sandiumenge, CrystEngComm **15**, 3908 (2013).

[29] J. Dho, N. H. Hur, I. S. Kim, and Y. K. Park, J. Appl. Phys. **94**, 7670 (2003).